THE ASTROPHYSICAL JOURNAL, 308:199–212, 1986 September 1

THE DISCOVERY OF 3.8 HOUR PERIODIC INTENSITY DIPS AND ECLIPSES FROM THE TRANSIENT LOW-MASS X-RAY BINARY EXO 0748−676

A. N. PARMAR,[1] N. E. WHITE,[1] P. GIOMMI,[1,2] AND M. GOTTWALD[1]
EXOSAT Observatory, Darmstadt
Received 1985 October 16; accepted 1986 February 19

ABSTRACT

Using the *EXOSAT* Observatory we have discovered a new transient X-ray burst source EXO 0748−676 that shows 8.3 minute duration X-ray eclipses that recur with a period of 3.82 hr. If the companion star is on the main sequence, the eclipse duration gives a companion mass of 0.45 $M_\odot$ and a system inclination of 75°. Irregular intensity dips that involve up to an 80% reduction in 2–10 keV intensity are observed at orbital phases between ~0.8–0.2 and at $\phi \approx 0.65$ (where center of eclipse corresponds to $\phi = 0.0$) with evidence for shallower dipping activity at other orbital phases. The intensity dips are most likely due to obscuration of the central X-ray source by a thickened region (or splash) at the outer edge of the accretion disk that is caused by its interaction with the inflowing gas stream. The dips are associated with an increase in absorption by material that has a metallicity a factor of 2–7 below solar values. The depth of the dip at $\phi \approx 0.65$ tends to be deeper when the overall source intensity is high. Residual emission is present during eclipse at a level of 4% of the 2–6 keV uneclipsed flux. This may be emission scattered into the line of sight by an accretion disk corona with a contribution below 2 keV from interstellar dust grains.

Subject headings: stars: eclipsing binaries — stars: individual — X-rays: binaries

I. INTRODUCTION

Several X-ray binary systems have been found to exhibit periodic irregular dips in X-ray intensity (White and Mason 1985 and references therein; van der Klis *et al.* 1985; Watson *et al.* 1985). The dip recurrence intervals range from 0.83 hr to 21 hr with a duty cycle of ~10%–20%. The duration, depth, and shape of each dipping interval can vary dramatically from cycle to cycle. Within each dipping interval the observed intensity varies erratically on a time scale of a few seconds (e.g., XB 1254−690; Courvoisier, Parmar, and Peacock 1984). The dips are more pronounced at low energies, indicative of photoelectric absorption (except those seen from X1755−338 which are energy independent; White *et al.* 1984).

The periodic nature of these dips combined with their energy dependence and irregular intensity variability suggests that they are caused by the obscuration of the central compact X-ray source by material in a thickened region at the edge of an accretion disk, the location of which is fixed in the reference frame of the binary (White and Swank 1982; Walter *et al.* 1982). This thickened region begins at the point where the gas stream from the lobe filling companion impacts the edge of the accretion disk and extents several tens of degrees downstream. Optical observations show periodic variations in intensity with the same period as the dip recurrence intervals (Motch *et al.* 1984; Mason, Parmar, and White 1985). The observed optical minima occur ~0.2 cycles after the center of the dipping activity. This is consistent with the expected position of the thickened region in the binary system if minimum light corresponds to viewing the varying aspect of an X-ray heated companion or the occulation of the edge of the accretion disk by the companion star.

The X-ray dipping sources are not the only LMXRB systems to show evidence for an orbital modulation. The partial eclipsing systems X1822−371 and XT 2129+470 each contain a thick azimuthally structured accretion disk that completely hides the central compact X-ray source from direct view. X-rays are scattered into the line of sight by an accretion disk corona (ADC) (White and Holt 1982; McClintock *et al.* 1982). A smooth variation in X-ray intensity with orbital phase is observed that precedes the partial eclipse of the ADC by the companion. The X-ray light curve of X1822−371 can be successfully modeled in terms of an accretion disk that is thickened at the point of impact of the gas stream from the companion (White and Holt 1982). This model can also explain the optical, ultraviolet, and infrared light curves (Mason and Córdova 1982).

In this paper we present the results of a series of *EXOSAT* observations designed to follow the evolution of the outburst of the recently discovered X-ray transient EXO 0748−676 (Parmar *et al.* 1985*b*). We report the detection of X-ray eclipses, intensity dips, and X-ray bursts as well as evidence for a region of extended emission. In § II we report the discovery of this source and subsequent observations. The properties of the X-ray eclipses are discussed in § III, and in § IV the energy dependence of the dips is investigated. The long-term evolution of the X-ray light curve is presented in § V. The transient nature of this source is considered in § VI, and the identification of the system briefly discussed in § VII. In § VIII we discuss the implications of these results for the nature of the dipping sources in general and compare the properties of EXO 0748−676 with those of the other dipping X-ray binary systems as well as with those systems where the observed X-rays are scattered into the line of sight by an ADC. A detailed description of the properties of the X-ray bursts is given elsewhere (Gottwald *et al.* 1986).

II. OBSERVATIONS

The observations presented here were obtained using a channel electron multiplier array detector (CMA; 0.04–2.0

[1] Affiliated to the Astrophysics Division, Space Science Department of ESA.
[2] On leave from CNR Istituto di Fisica Cosmica, Milano.

keV; de Korte *et al.* 1981) behind a low-energy imaging telescope and a 3000 Å Lexan filter, the medium energy proportional counter array (ME; Turner, Smith, and Zimmermann 1981), and gas scintillation proportional counter (GSPC; Peacock *et al.* 1981) on the European Space Agency's *EXOSAT Observatory*. All three instruments have overlapping fields of view and were used simultaneously.

The ME consists of eight gas-filled proportional counters, each containing an argon (1–15 keV) and xenon (5–55 keV) chamber. Half of the counters were pointed directly at EXO 0748−676 to provide an effective area of ~ 700 cm^2. The other counters were pointed at a nearby source-free region of sky to provide a simultaneous background monitor, and all ME count rates quoted here are for one-half of the counters observing the source. To optimize the background subtraction, the pointing directions of the array halves were exchanged every ~ 4 hr. For most of the observations 64 channel pulse height analyser spectra were obtained for both the argon and xenon counters at 1 s intervals.

EXOSAT spends ~ 25% of its time maneuvering between different X-ray sources. During these intervals the ME and GSPC instruments are still operated to monitor the background counting rate and to observe X-ray sources that pass through the 45′ fields of view of the instruments. The usual maneuvering rate of 44° hr^{-1} gives an effective exposure time for a compact X-ray source of ~ 1 minute. This provides a powerful means of discovering bright uncataloged X-ray sources as well as monitoring the activity of known X-ray sources. During such a maneuver on 1985 February 11 at 1755 UT a bright, ~ 50 counts s^{-1} (1 ME count s^{-1} corresponds to 1.15×10^{-11} ergs cm^{-2} s^{-1} for a power-law spectrum with photon index 2.1 and equivalent low-energy absorption [$N_{\rm H}$] of 3×10^{21} H cm^{-2}; 2–10 keV), new X-ray source was detected in the ME and positioned to an accuracy of $\sim 15'$. A follow-up pointed *EXOSAT* observation on 1985 February 15 using the CMA gave a position for this source of R.A. $07^{\rm h}48^{\rm m}24^{\rm s}.5$, decl. $-67°37'23''$ (epoch 1950) with an uncertainty radius of 15″ (Pamar *et al.* 1985*b*).

The 1–10 keV ME light curve obtained during this observation is shown in Figure 1. In addition to four X-ray bursts, the light curve shows a remarkable amount of structure with 3.8 hr periodic eclipses and irregular intensity dips visible. The depth and occurrence times of the dips can be seen to vary from cycle to cycle. The ME light curves obtained during three other *EXOSAT* observations of EXO 0748−676 are shown in Gottwald *et al.* (1986). During the 1985 July 19 observation the ME was operated in a mode that provided 1–15 keV intensity samples every 2 ms. An unsuccessful search for periodicities and quasi-periodic oscillations was made using this data down to a time scale of 4 ms (L. Stella 1985, private communication).

A total of eight *EXOSAT* observations of EXO 0748−676 were made between 1985 February 15 and July 19 with durations that varied between 6.2 and 24.0 hr (Table 1). The overall 1–10 keV count rate, corrected for collimator transmission during dip, eclipse, and burst-free intervals for each observation, is shown in Figure 2. Following the first two *EXOSAT* observations on 1985 February 15 and 18, the observed count rate declined by a factor of 3 from ~ 50 counts s^{-1} to ~ 15 counts s^{-1}. During the last two *EXOSAT* observations EXO 0748−676 was observed to be brighter than seen before, at ~ 80 counts s^{-1} suggesting that it may be a long-lived X-ray source.

The ME spectrum of EXO 0748−676 obtained when the source was not bursting, eclipsing or dipping (hereafter referred to as the quiescent spectrum) during the first *EXOSAT* observation could not be well fitted by either power law (χ^2 of 116 for 42 degrees of freedom [dof] with a best fitting photon index of 2.4) or thermal bremsstrahlung models (χ^2 of 116 for 42 dof with a best fitting temperature, kT, of 5.3 keV). Fitting to a power law with an exponential cutoff model: $S = A.E^{-\Gamma} \cdot \exp(-E/kT)$ photons cm^{-2} s^{-1} keV^{-1}, where E is energy in keV with an $N_{\rm H}$ of $(7.8 \pm 1.0) \times 10^{21}$ H cm^{-2} gave a good fit with a χ^2 of 41 for 41 dof. The best fit value of Γ is 1.92 ± 0.12 and $kT = 11.1^{+3.5}_{-2.0}$ keV (all uncertainties are 90% confidence). A 1% systematic uncertainty was included in the fitting to account for uncertainties in the detector calibration. The 90% confidence upper limit to any 1 keV full width half-maximum emission feature between 6.4 and 6.7 keV obtained using the GSPC is 40 eV during the 1985 June 1 observation.

The results of spectral fits to the ME data from the other

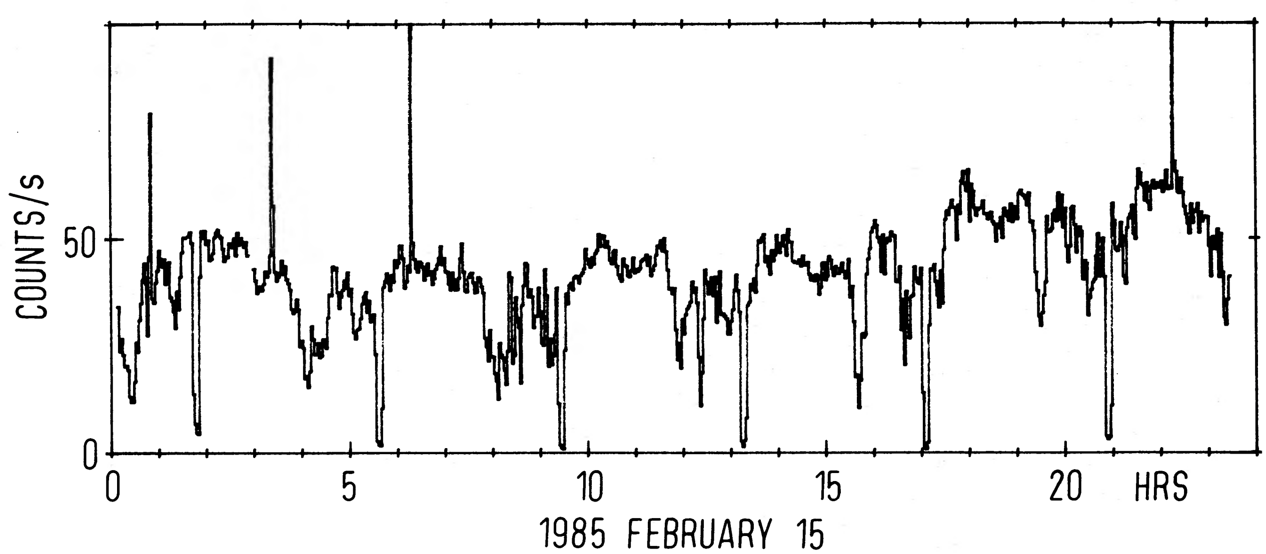

FIG. 1.—The ME 1–10 keV background subtracted light curve of the 1985 February 15 observation of EXO 0748−676 plotted with a time resolution of 125 s. Periodic eclipses, irregular intensity dips, and four X-ray bursts are visible.

TABLE 1

SPECTRAL ANALYSIS

OBSERVATION START DATE (1983)	DURATION (hr)	SPECTRAL PARAMETERS Γ	kT	N_H[b]	FLUX[a]	χ^2/dof
Feb 15.0	24.0	1.92 ± 0.12	$11.1^{+3.5}_{-2.0}$	0.78 ± 0.10	8.9	41/41
Feb 18.9	17.7	$2.05^{+0.15}_{-0.20}$	$14.0^{+9.0}_{-5.0}$	0.92 ± 0.15	9.2	29/32
Feb 26.1	17.3	2.25 ± 0.04	...	0.58 ± 0.15	4.8	29/31
Mar 10.3	8.3	0.20 ± 0.20	5.1 ± 2.2	$0.20^{+0.50}_{-0.20}$	3.0	27/28
Mar 28.8	9.9	0.80 ± 0.30	20^{+100}_{-10}	$0.90^{+0.60}_{-0.10}$	4.6	45/31
Apr 8.9	7.7	-0.28 ± 0.31	$4.0^{+2.5}_{-0.7}$	$0.25^{+1.00}_{-0.25}$	3.1	10/12
Jun 1.2	12.7	1.06 ± 0.14	4.6 ± 0.5	0.18 ± 0.14	15.0	34/36
Jul 19.7	6.2	1.32 ± 0.15	$4.6^{+0.8}_{-0.6}$	0.56 ± 0.16	10.5	17/16

NOTE.—All uncertainties are 90% confidence.

[a] For nondip, burst, or eclipse intervals integrated over the entire observation between 1 and 20 keV in units of 10^{-10} ergs cm^{-2} s^{-1}.

[b] In units of 10^{22} H cm^{-2}.

observations during quiescent intervals are shown in Table 1. These spectra could be satisfactorily fitted with the above model except for the 1985 February 26 observation where a single power-law model with $\Gamma = 2.25 \pm 0.04$ was satisfactory. There is evidence that the spectrum varies from observation to the next from these fits with Γ varying between -0.3 and 2.3 and kT varying from ~ 11 to ~ 4 keV. There is no obvious relation between these changes in spectrum and the overall flux or evolution of the outburst. These spectral fits are similar to those of other X-ray burst sources that have been studied in detail (e.g., White and Mason 1985). For an assumed distance of 10 kpc the 2–10 keV quiescent luminosity of EXO 0748−676 varied between $\sim 1.3 \times 10^{37}$ ergs s^{-1} and $\sim 2.3 \times 10^{36}$ ergs s^{-1} during the 1985 June 12 and March 10 observations respectively. The actual distance is not known although the X-ray bursts suggest it to be ~ 10 kpc (Gottwald *et al.* 1986).

III. THE X-RAY ECLIPSES

Using the eclipse ingresses and egresses as fiducial markers we derived an orbital period of $3.82410725 \pm 0.00000075$ hr (90% confidence) with center of eclipse occurring at JD $2{,}446{,}111.574550 \pm 0.000025$ (barycentric). The mean eclipse duration is 0.1390 ± 0.0003 hr, which corresponds to an eclipse semi-angle of $6.^{\circ}543 \pm 0.^{\circ}015$. Using this ephemeris we folded the ME background-subtracted data from nine of the eclipses observed during the first two *EXOSAT* observations (Fig. 3). The eclipses are not total with an average of $4.2\% \pm 0.3\%$ of the uneclipsed 2–6 keV intensity remaining. The intensity of this residual emission is linearly correlated (with a correlation coefficient of 0.94 for 19 dof) with the average strength of the uneclipsed intensity observed during the intervals preceding and following the eclipses (Fig. 4).

Figure 3 shows that the eclipse ingress and egress are resolved in the ME data and have a duration of ~ 6 s. In addition there is evidence for a slight shoulder just before and after ingress (and egress) suggesting the presence of a second extended component. An ME spectrum obtained by integrating 3 s intervals of data obtained during the eclipse transitions observed during the 1985 February 15 and 18 observations shows evidence for an increase in N_H from $(1.6 \pm 0.3) \times 10^{22}$ H cm^{-2} seen during nearby dipping intervals to $(2.8 \pm 0.6) \times 10^{22}$ H cm^{-2}. This suggests that we are seeing absorption effects in the atmosphere of the companion star.

A CMA image obtained by summing data from 18 eclipses

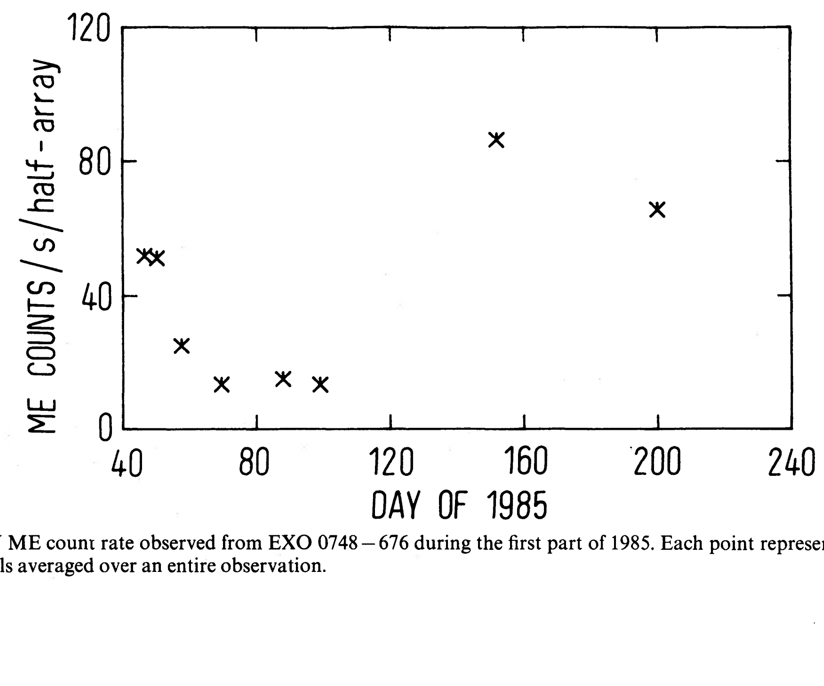

FIG. 2.—The overall 1–10 keV ME count rate observed from EXO 0748−676 during the first part of 1985. Each point represents the count rate obtained during dip, eclipse, and burst-free intervals averaged over an entire observation.

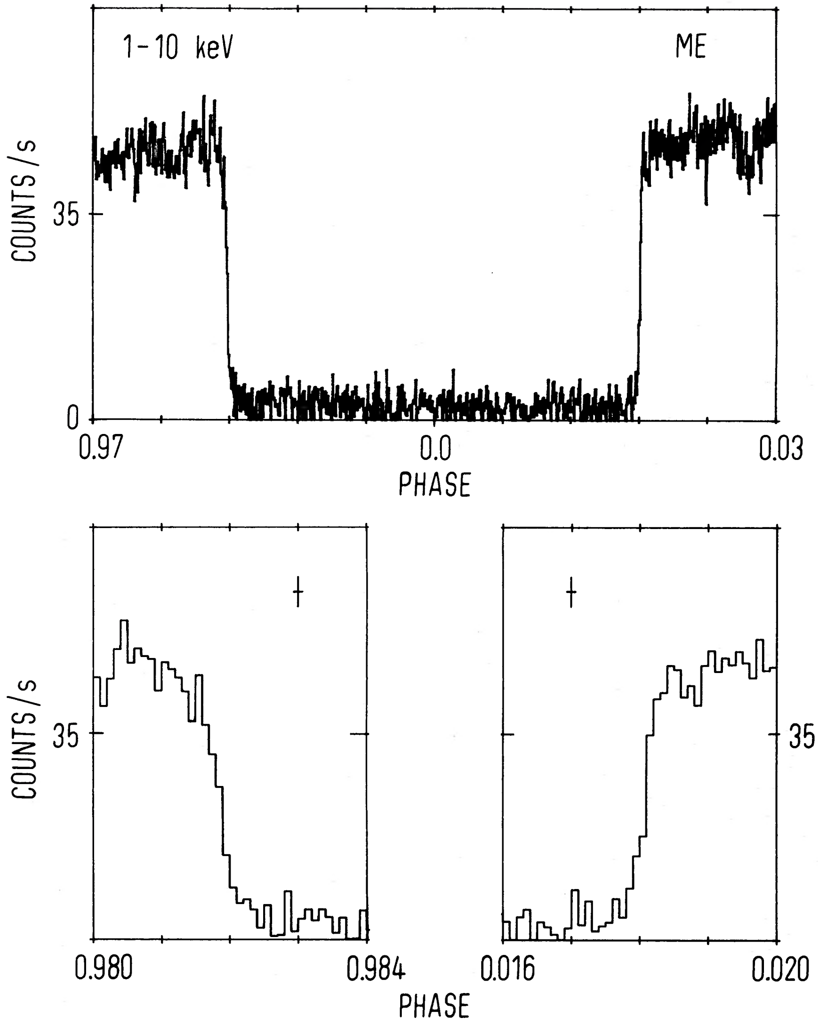

FIG. 3.—The upper panel shows the the ME 1–10 keV background-subtracted light curve of nine eclipses observed during the first two *EXOSAT* observations folded using the ephemeris given in the text. Each bin corresponds to an interval of 1.4 s. The lower panel shows the ingress and egress in greater detail with the same time resolution. The error bars represent 1 σ statistical uncertainties.

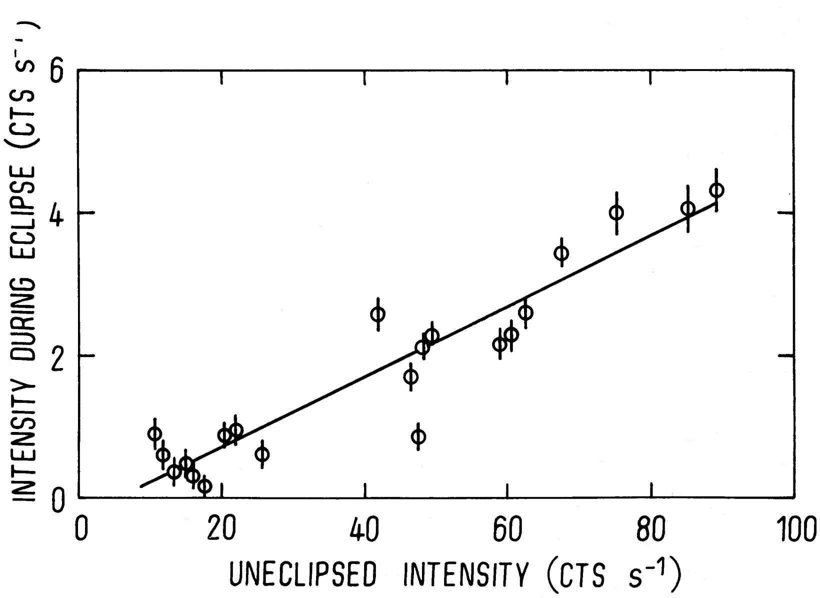

FIG. 4.—The ME 2–6 keV count rate during eclipse plotted against the count rate taken from nearby uneclipsed intervals. The straight line shows the best fitting linear relation with slope 0.049 ± 0.004 and intercept -0.30 ± 0.20.

where good CMA and ME coverage was available gives a count rate of 0.025 ± 0.003 counts s^{-1} at the expected position of EXO 0748−676. This represents $7.4\% \pm 0.8\%$ of the quiescent flux and is significantly larger than the residual count rate observed in the ME. This additional flux may come from scattering off interstellar dust grains (Overbeck 1965). This would lead to a broader point-spread function in the imaging CMA than observed from a point source. There is some evidence that during eclipsing intervals the distribution of counts with position is indeed broader than expected from a point source. However only ~ 100 counts were detected during eclipses, and we cannot rule out that this apparent extent is due to systematic uncertainties in background subtraction.

The ME spectrum accumulated over the same eclipses used above is shown in Figure 5, along with the CMA measurement. The total integration interval is 1.7 hr. A good fit can be obtained to the combined ME and CMA data using a single power-law model with photon index of 2.2 ± 0.2 and N_H of $(1.8 \pm 0.7) \times 10^{21}$ H cm^{-2} for a χ^2 of 17 for 17 dof. In order to see if the shape of this spectrum is consistent with that of the quiescent emission, we fitted a power law with exponential cutoff model with kT, Γ, and N_H fixed at the best fitting values from the quiescent spectrum of the 1985 February 15 observation (Table 1) to these data. The model fits the data well at energies >2 keV, but below this energy there is a significant excess of observed counts over that predicted resulting in a χ^2 of 85 for 19 dof. Using the spectral parameters derived from the other observations does not produce significantly better fits. This low-energy excess can be modeled as a power-law component with N_H fixed at the quiescent value and photon index 6.3 ± 0.8 allowing a good fit to be obtained at energies <2 keV with an overall χ^2 of 15 for 17 dof. Between 2 and 6 keV, this power-law component is responsible for 0.057 ± 0.013 of the total emission seen during eclipse, while in the 0.04–2.0 keV passband of the CMA, it contributes 0.82 ± 0.19 of the observed counts, and is consistent with the excess residual emission seen in the CMA.

IV. THE ENERGY DEPENDENCE OF THE X-RAY DIPS

Figure 6 shows the ME 1–10 keV light curve of ~ 4 hr of data from EXO 0748−676 obtained on 1985 February 15. The hardness ratio is obtained from the counts in the 4–10 keV band divided by those in the 1–4 keV band. Two eclipses are visible centered on 0926 UT and 1316 UT. Figure 6 illustrates how the hardness ratio can be used to distinguish between intrinsic source variability and dipping activity. During the nondipping intervals the observed intensity variability appears to be energy independent, while during dipping intervals there is a marked increase in hardness ratio.

In order to investigate the X-ray spectrum during dipping intervals a series of intensity-selected ME spectra were accumulated using data obtained during the dips observed during the 1985 February 15 and 18 observations. No attempt was made to correct for long-term variations in the nondip source intensity. Since the shape of the quiescent spectrum of EXO 0748−676 does not vary significantly on a time scale of hours

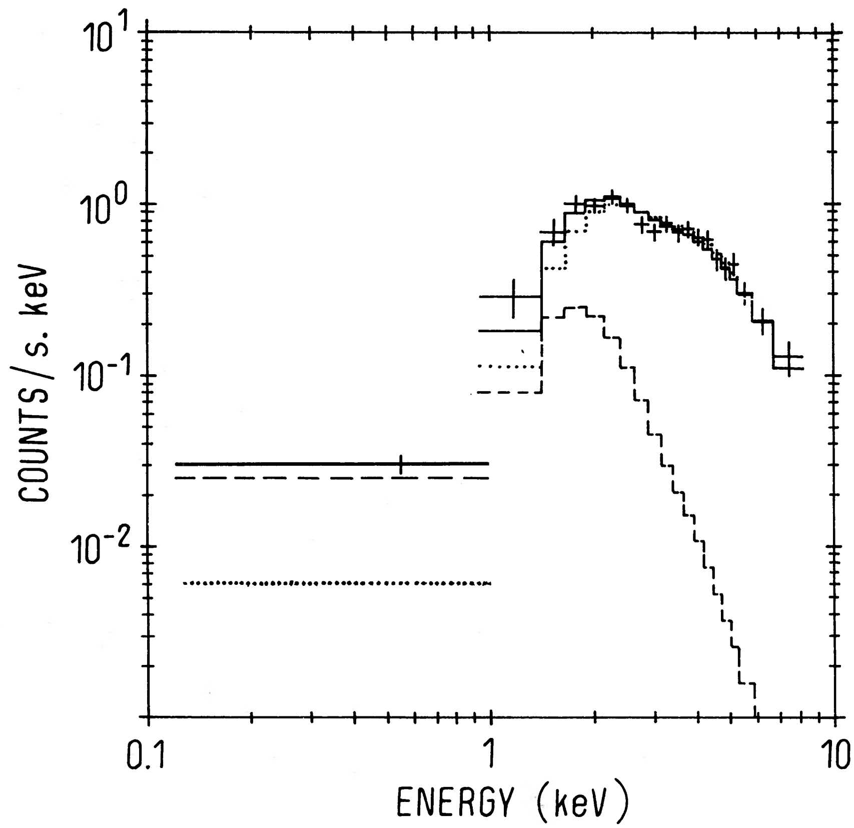

FIG. 5.—The ME spectrum and CMA measurement obtained by integrating data over 18 eclipses of EXO 0748−676. The histogram shows the sum of the best fitting power law with an exponential cutoff model fit with Γ, kT, and N_H fixed at their quiescent values and a separate power-law component needed to provide a good fit at energies <2 keV. The dotted and dashed line histograms indicate the contribution of the power law with exponential cutoff and soft power law components respectively.

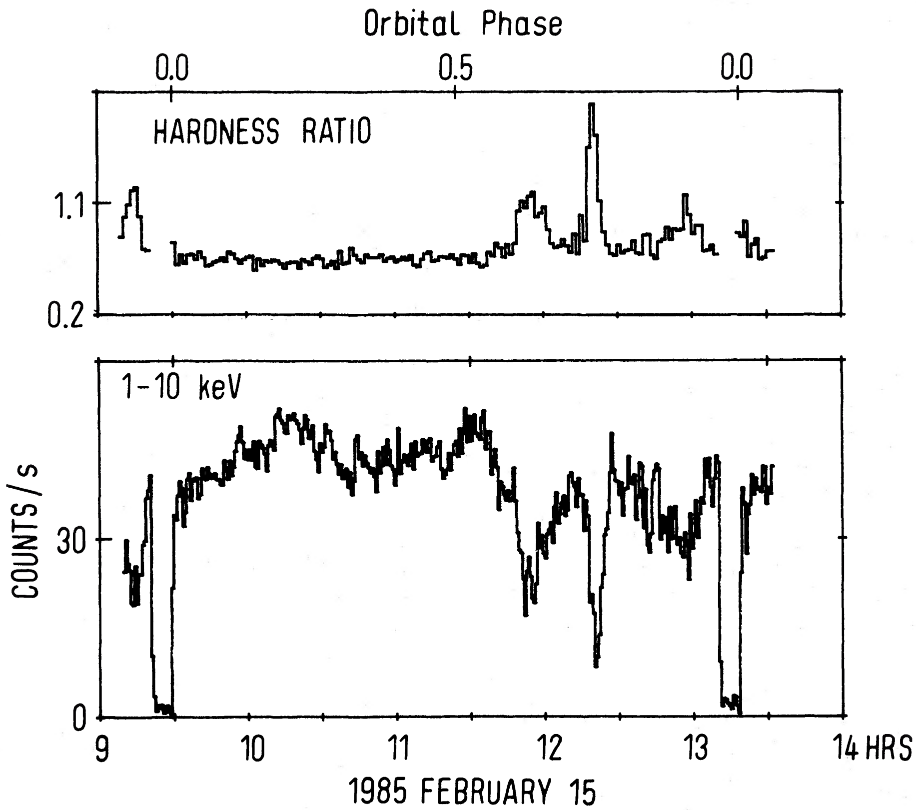

FIG. 6.—The ME 1–10 keV light curve and hardness ratio (defined as the counts in the band 4–10 keV divided by those in the 1–4 keV band) for ~4 hr of data from EXO 0748 − 676 during the 1985 February 15 observation.

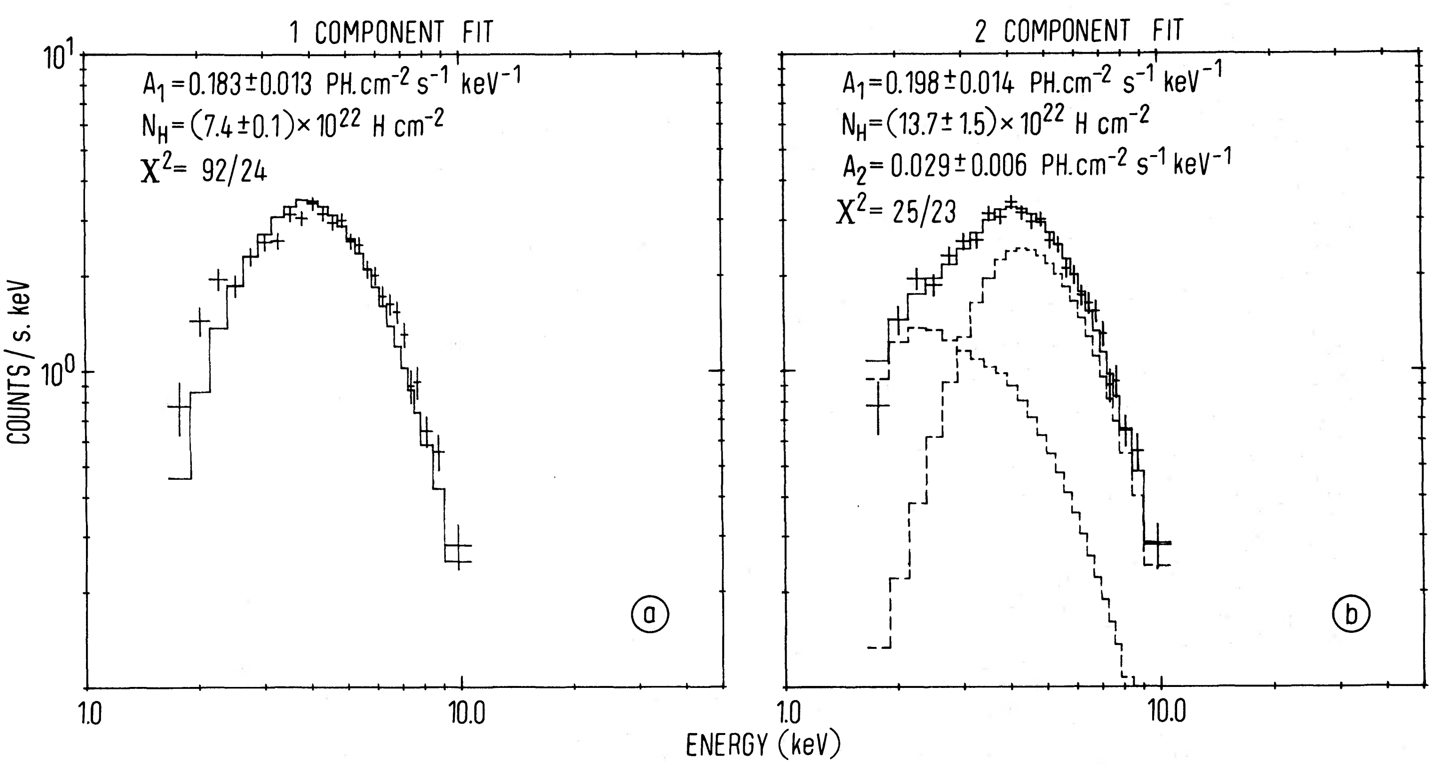

FIG. 7.—The results of fitting a representative ME dip spectrum to one-component (*a*) and two-component (*b*) power law with exponential cutoff models. The method of obtaining the spectrum is given in the text. Γ, kT, and N_H were fixed at the best fitting quiescent spectrum values of 1.92, 11.1 keV, and 7.8 × 10^{21} H cm^{-2}, respectively. The dashed lines indicate the contributions of the fixed absorption component, which contributes more flux at energies <3 keV, and the variable absorption component.

(e.g., Fig. 6), the power law with an exponential cutoff model discussed earlier was fitted to the dip spectra keeping Γ and kT fixed at their quiescent values (Table 1). Photoelectric absorption by cold material will then be seen as an increase in N_H while electron scattering, which is energy independent, will be seen as a reduction in A.

An example of this fitting procedure is shown in Figure 7*a* for a spectrum obtained by integrating ME data with a 2–6 keV count rate of between 20 and 25 counts s^{-1} (before background subtraction which contributes 10 counts s^{-1}). The total integration time is 800 s. The best fitting model indicates a factor of 9 increase in N_H to 7.1×10^{22} H cm^{-2}, but gives a poor χ^2 of 92 for 24 dof because of an excess of counts at low energies. Since the excess flux seen during eclipse indicates that a component with low absorption is present, a second component with variable normalization but with N_H, Γ, and kT fixed at the quiescent spectrum values given in Table 1 was included in the model. A good fit is now obtained with a χ^2 of 25 for 23 dof. The variable absorption component has an N_H of $(1.37 \pm 0.15) \times 10^{23}$ H cm^{-2}. Figure 7*b* shows the result of this fit with the contributions of the two components indicated separately as dashed histograms. Since the eclipse spectrum can also be represented by a power-law model with photon index 2.2, we also fitted this spectrum, in conjunction with the quiescent spectrum described above, to the dip spectrum. A good fit was obtained with a χ^2 of 26 for 23 dof. The N_H of the variable absorption component is now $(1.20 \pm 0.15) \times 10^{23}$ H cm^{-2}. Since both models for the low-energy excess give similar values of χ^2 and N_H we will use the power law with exponential cutoff form to model the low-energy excess in the analysis of the dip spectra that follows.

Figure 8 illustrates the results of fitting this two-component model to the intensity selected dip spectra. Figure 8*a* shows the increase in N_H with dip depth, and Figures 8*b* and 8*c*, the variation in the normalization, A, of the variable and fixed absorption components with count rate, renormalized such that unity represents the value of the nondip spectrum. Figures 8*a* and 8*c* include two points derived from measurements in quiescence. The normalization of the fixed low-absorption component decreases with increasing dipping activity (or decreasing count rate) and, during intervals when the dipping activity is most intense, is of similar intensity to the emission seen during eclipse (0.042 ± 0.003). However, fixing the normalization of the low-absorption component at this value does not give a good fit at all intensity levels through the dips. The normalization of the variable absorption component remains approximately constant throughout the dips.

The large uncertainties in the parameters of the two-component fits for spectra obtained near the top of dips reflects the fact that a single-component model with a small increase in N_H is an adequate fit to the data. The two components in this case simply trade off against one another. This suggests that the reduction in normalization of the fixed N_H component observed during intervalss of low N_H may be caused by the contributions of the two components not being well separated. The dashed vertical line in Figure 8 indicates approximately where the average reduced χ^2 of the one-component fits rises above 2 as the count rate decreases. During moderately intense dipping intervals, where the count rate is between 20 and 40 counts s^{-1}, the contributions of the two components are well separated, and good fits cannot be obtained using single-component models. During these intervals the normalization of the fixed absorption component can be as high as $\sim 20\%$ of that of the quiescent spectrum. In this count rate range, intrinsic variations in the source intensity will be important and, as will be discussed later, will give rise to such an effect.

The intensity-selected dip spectra are not of sufficient quality to rule out a number of different models for the low-energy excess. An example of such a model that has the same number of fitted parameters as the two component model presented above is the "clumpy cloud" model discussed in Nagase (1985). In this model the photoelectric absorption which is normally expressed as $\exp(-N_H \cdot \sigma_{MM})$, where σ_{MM} are the absorption coefficients of Morisson and McCammon (1983) is given by $\exp\{-\nu[1 - \exp(-\sigma_{MM} \cdot N_c)]\}$, and the number of clouds in the line of sight is assumed to be given by a Poisson distribution with mean ν. Each cloud has an average column density N_c. Acceptable fits are obtained to the spectra with a similar goodness of fit as with the two-component model. The best fit value of ν varies between ~ 1 and ~ 3 and N_c between $\sim 5 \times 10^{21}$ and $\sim 5 \times 10^{22}$ H cm^{-2}. Both types of fit show similar reductions in spectral normalization during intervals of intense dipping activity.

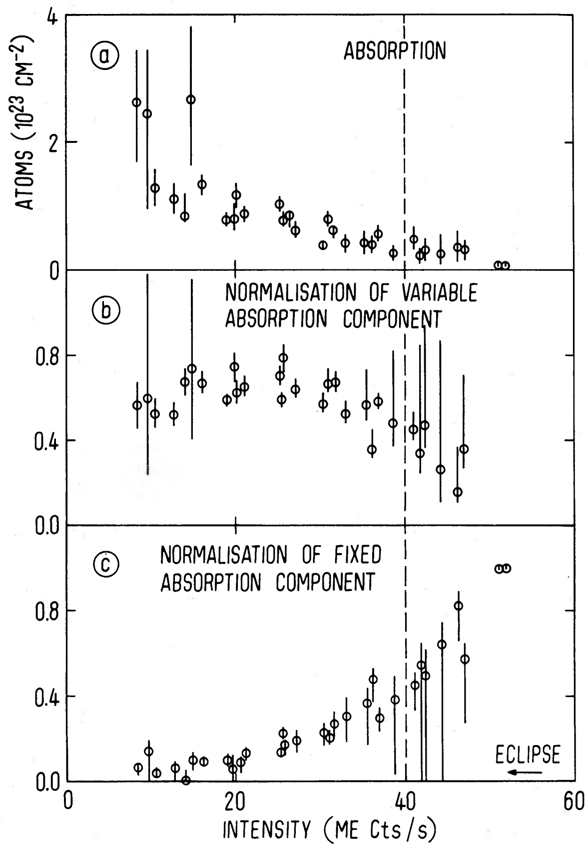

FIG. 8.—The results of two-component spectral fits to the intensity-selected dip spectra discussed in the text. Both components have their temperatures and power-law indices fixed at the quiescent values, while one component also has its absorption fixed at the quiescent value. Fig. 8*a* shows the best fitting low-energy absorption; Fig. 8*b* shows the normalization of the variable absorption component; and Fig. 8*c* shows the normalization of the fixed absorption component against count rate, respectively. Figs. 8*b* and 8*c* are scaled such that 1.0 represents the normalization of the quiescent spectrum. The dashed vertical line indicates the approximate region where the reduced χ^2 of a single component fit rises to 2 as the count rate decreases. The intensity of emission observed in eclipse by the ME is shown in Fig. 8*c*.

In order to investigate the time scales of variability during dipping intervals, we constructed the autocorrelation function (ACF) of 400 s intervals of 1–10 keV ME data obtained with a time resolution of 1 s. The effects of long-term intrinsic source variability on the ACF were removed by dividing the data by a fourth-order polynomial fit before calculating the ACF. The exponential decay of the ACF gives a characteristic time scale for the intensity variability during the dips of ~ 15 s with evidence for variability on time scales as short as 1 s.

V. THE EVOLUTION OF THE X-RAY LIGHT CURVE

Figures 9*a* and 9*b* show the ME light curve and hardness ratio for each observation of EXO 0748$-$676 obtained by folding over the ephemeris given above with the eclipses centered on $\phi = 0$. The plot is repeated over half a cycle for clarity. Intervals where X-ray bursts occurred are excluded. Intervals during which there was dipping activity present are most easily seen as increases in hardness ratio. The maximum reduction in 1–10 keV intensity during the dips is $\sim 80\%$.

The structure of the light curve changed as the outburst evolved. During the 1985 February 15 observation two deep broad dips were visible centered on $\phi \approx 0.65$ and $\phi \approx 0.90$. In the following observations, as the overall intensity decayed, the dip at $\phi \approx 0.65$ became narrower and less deep such that it was almost undetectable by the time of the 1985 April 8 observation. The dip at $\phi \approx 0.9$ appeared to become weaker between the 1985 February 15 and 1985 March 10 observations. However, during the next observation, on 1985 March 28 two deep dips centered on $\phi \approx 0.90$ and $\phi \approx 0.10$ were present. These dips are visible throughout the remaining observations. During the 1985 June 2 and July 19 observations where EXO 0748$-$676 was at its brightest observed intensity, the dip at $\phi \approx 0.65$ was once again present suggesting that the depth of this dip may be related to source intensity and hence accretion rate. It is possible that there was a small amount of dipping activity present between $\phi \approx 0.40$ and $\phi \approx 0.15$ during the 1985 February 15 observation although it is difficult to distinguish between low-level dipping activity and intrinsic spectral changes.

VI. THE TRANSIENT NATURE OF EXO 0748$-$676

Previous all-sky X-ray surveys by the *Uhuru*, *Ariel V*, and *HEAO 1* satellites did not detect EXO 0748$-$676 (Forman *et al.* 1978; McHardy *et al.* 1981; Wood *et al.* 1984). This source, located at $l = 280.0$, $b = -19.8$ is in an unabsorbed part of the sky with no bright X-ray sources nearby that might cause source confusion. Had it been present at the intensity seen by *EXOSAT*, it would have been easily detected.

An *Einstein* Imaging Proportional Counter (IPC) observation of the nearby star L97–12 on 1980 May 22 included the position of EXO 0748$-$676 at a location 22′ from the center of the field of view. A source was detected at a position consistent with that of EXO 0748$-$676 with a count rate of 0.020 ± 0.003 counts s^{-1} in the 0.2–3.5 keV band. Assuming a power-law spectrum with photon index 2.2 and an N_H of 5×10^{21} H cm^{-2}, this corresponds to flux of 6.3×10^{-13} ergs cm^{-2} s^{-1}, giving an unabsorbed luminosity of 1.2×10^{34} ergs s^{-1} for an assumed distance of 10 kpc. There is no evidence for any large changes in source intensity during the 2.9 hr observation which started at $\phi = 0.10$ but did not include an eclipse interval. The lowest 0.2–3.5 keV luminosity observed by *EXOSAT* from EXO 0748$-$676 during nondip and noneclipse intervals was 8.2×10^{35} ergs s^{-1} during the 1985 March 10 observation. This corresponds to a luminosity during eclipse of 3.5×10^{34} ergs s^{-1} which is a factor of 3 more than the *Einstein* detection.

Finally, we note that *SAS 3* observed a burst from the region of sky containing EXO 0748$-$676 (Doty 1976). However the large *SAS 3* error region of $\sim 24°$ by 24° includes 10 of the sources in the fourth *Uhuru* catalog (Forman *et al.* 1978), so it is possible that the observed burst was from another object.

VII. THE OPTICAL COUNTERPART

EXO 0748$-$676 was identified by Pedersen and Mayor (1985) to be coincident with a blue $m_v = 16.9$ object. During 1985 February this object showed a 3.8 hr modulation in its light curve as well as a broad ~ 30 minute duration minimum centred on the time of X-ray eclipse with a reduction in flux of $\sim 25\%$ (Pedersen *et al.* 1985; Wade *et al.* 1985). The optical light curve varies erratically from orbit to orbit. The position of the optical object is R.A. $07^h48^m24^s.90 \pm 0^s.20$, decl. $-67°37'32''.3 \pm 1''.0$ (epoch 1950; Pedersen *et al.* 1985) which is 10″ from the center of the 15″ radius uncertainty region of Parmar *et al.* (1985*b*). The optical spectrum shows a blue continuum with emission lines of H and He II 4686 Å, characteristic of LMXRB systems (Pedersen *et al.* 1985; Mouchet, Angebault, and Ilovaisky 1985; Crampton *et al.* 1986).

VIII. DISCUSSION

a) System Parameters

The detection of both eclipses and dips that recur with the orbital period from EXO 0748$-$676 confirms the scenario for X-ray dips first discussed by White and Swank (1982) and Walter *et al.* (1982). In this the dips are caused by obscuration of a central compact X-ray source by material in a thickened region at the edge of the accretion disk, the thickened region being caused by the impact of the gas stream from the companion star on the accretion disk. These observations allow the relative phase of the thickened region to the overall binary geometry to be unambiguously determined. The tendency for the dipping activity to be deepest between $\phi \approx 0.5$ and $\phi \approx 1.0$ corresponds to viewing the region of the accretion disk where the interaction with the gas stream is expected to be largest. The duty cycle of the dipping behavior of up to $\sim 50\%$ is much larger than that normally seen from these dipping systems, where it is typically $\sim 10\%$–20%. This probably reflects the higher inclination of this system (see below). These observations also show that the orbital phase at which the deepest dips occur can change on a time scale of weeks making it is difficult to precisely estimate an underlying orbital ephemeris using dips as fiducial markers.

Combining Kepler's law and the Roche geometry (e.g., Paczyński 1971) and assuming that $M_{opt}/M_x < 0.8$ (where M_{opt} is the mass of the companion and M_x is the mass of the compact object) gives $R_{opt}{}^3 = 0.013 M_{opt} P^2$, where R_{opt} is the radius of the companion and P is the orbital period in hours. Combining the Roche relation with the measured eclipse duration enables the allowed range of M_{opt} as a function of system inclination angle to be estimated for different assumed values of M_x (Fig. 10). For a 1.4 $M_\odot$ compact object, the mass of a star that obeys the main-sequence mass-radius relation of Whyte and Eggleton (1980) and just fills its Roche lobe is 0.45 $M_\odot$. This gives a system inclination angle of 75°. The companion would then be an M dwarf. Relaxing the assumption that the companion is on the main sequence to the minimum possible companion mass, given by the point where the star

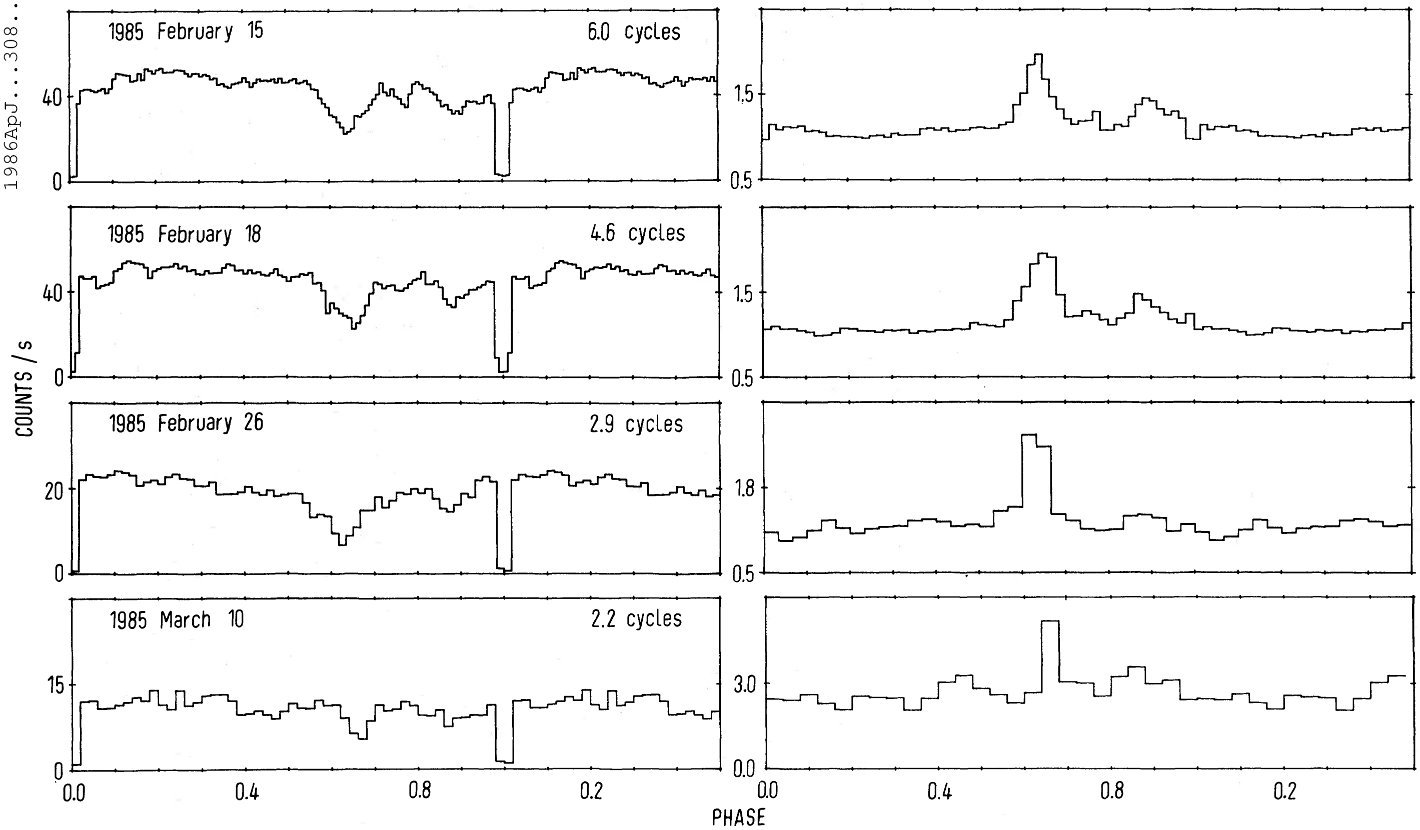

FIG. 9a

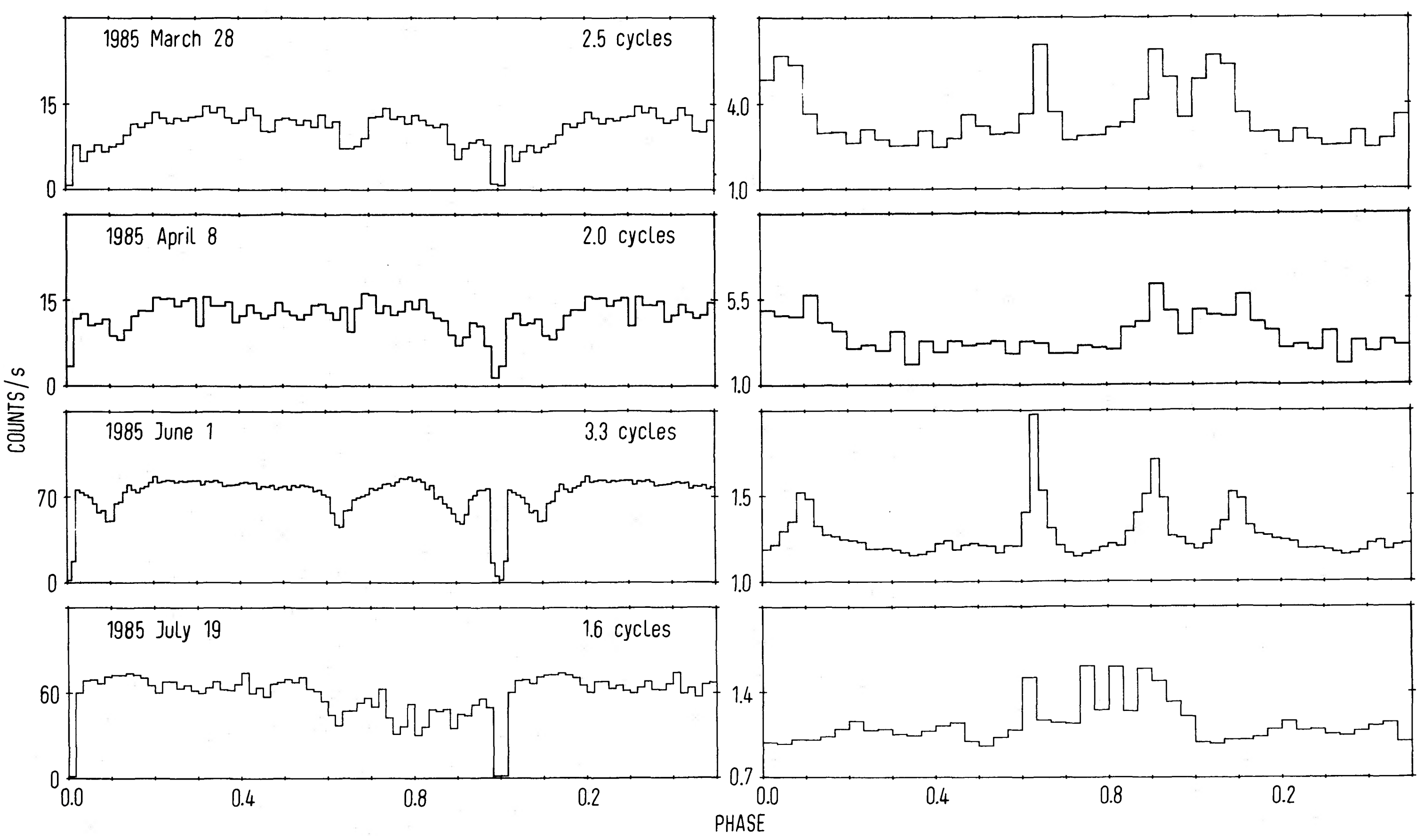

FIG. 9b

FIG. 9.—The ME 1–10 keV folded light curves and hardness ratios (defined as in Fig. 6) for the first (Fig. 9a) and second (Fig. 9b) four observations of EXO 0748 − 676. The folding ephemeris is given in the text.

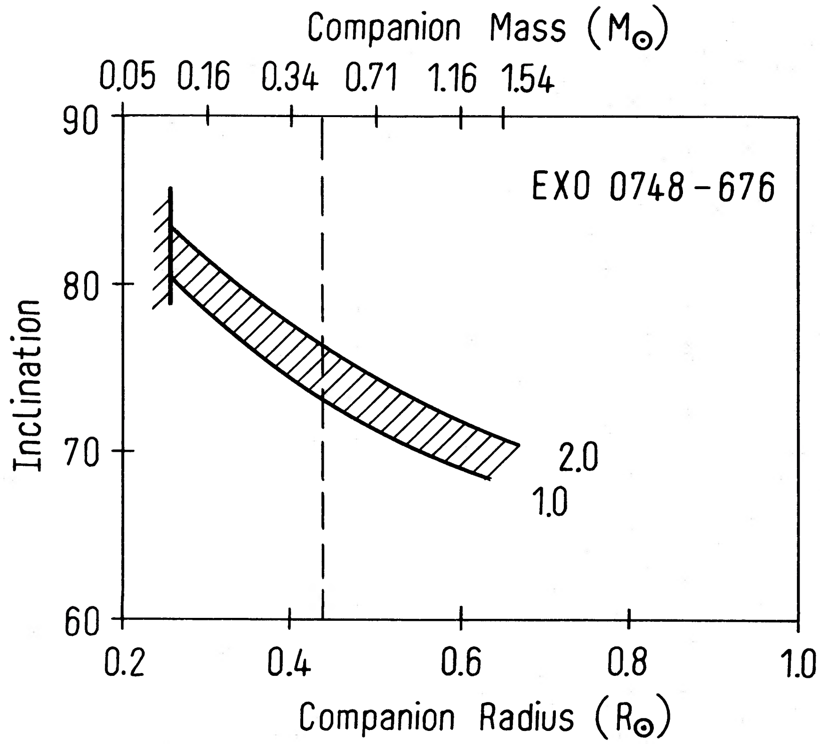

FIG. 10.—Allowed values of the companion radius and mass and system inclination for a range of assumed masses of the compact object in the EXO 0748 − 676 system between 1 and 2 $M_{\odot}$. The dashed vertical line indicates the mass-radius relation expected for a main sequence companion.

becomes degenerate (0.085 $M_{\odot}$), yields a maximum inclination angle of 82° for a 1.4 $M_{\odot}$ compact object. The companion mass probably lies somewhere between these two extremes. The system inclination angles and companion masses determined in this way are not very sensitive to the assumed value of M_x, e.g., for assumed values of M_x of 1 and 2 $M_{\odot}$ the difference in calculated inclination angles is $\pm 2°$ and in the companion masses ± 0.03 $M_{\odot}$. Thus the structure at the edge of the accretion disk must subtend an angle of between 8° and 15° above the plane of the orbit in order to obscure our line of sight and cause the dipping behavior as well as extending of order 180° around the edge of the disk.

b) *Scattered Emission*

The eclipses observed from EXO 0748 − 676 are not total with ~4% of the 2–6 keV uneclipsed intensity remaining. The spectrum of this residual emission can be interpreted as being from two components; the first contributing mainly at energies <2 keV and having a very soft spectrum and the second at energies >2 keV and having a spectrum similar to that of the quiescent emission.

It is natural to identify these components with emission regions already detected in other LMXRB systems. It is likely that the soft component is from X-rays scattered off interstellar dust grains. X-ray haloes around bright sources have already been detected by Rolf (1983), Catura (1983), Mauche and Gorenstein (1986), and Bode *et al.* (1985) using the *Einstein* IPC and high-resolution imager instruments which they interpret as being due to scattering from interstellar dust grains. For distant sources lying close to the galactic plane such as Cygnus X-3 ($l = 79.9$, $b = 0.7$), the fractional halo intensity in the IPC passband is 0.28 ± 0.03, whereas for 3C 273 at $l = 290$, $b = 64.5$ it is 0.04 ± 0.02 (Mauche and Gorenstein 1985). Xu, McCray, and Kelley (1986) point out that following an eclipse of a compact X-ray binary the halo should persist for several hours allowing it to be observed without the contaminating effect of the compact source being present. The cross section for the scattering of medium-energy X-rays by grains is proportional to E^{-2} implying that the halo spectrum should be much softer than the uneclipsed spectrum. This is consistent with the observed shape of the soft component seen in eclipse from EXO 0748 − 676.

The component that contributes most of the flux observed during eclipse at energies >2 keV is almost certainly scattered emission from an ADC since its spectrum is similar to that of the quiescent emission. Gottwald *et al.* (1986) have analyzed 22 type I X-ray bursts from this source. Of these, four bursts were recorded with a separation of 10–20 minutes. The second bursts of these pairs are a factor of ~3 fainter than the first burst. Shortly after an eclipse on 1985 March 28, an X-ray burst was observed at 1945 UT with properties similar to those of the second burst in a pair. An increase in count rate is visible during the preceding eclipse with a total count of ~300, ~4% of that expected from a first burst of a pair (cf. Fig. 5 of Gottwald *et al.* 1986). This is similar to the fractional residual count rate seen during eclipse. The duration of the burst observed during eclipse of ~2 minutes allows us to place an upper limit on the radius of the scattering region of $\sim 2 \times 10^{12}$ cm. This is consistent with the size of the ADC which is expected to have comparable dimensions to that of the accretion disk ($\sim 5 \times 10^{10}$ cm).

The X-ray spectra obtained during dips show a low-energy excess when compared to quiescent spectra and cannot be well fitted by a single-component model. During intervals where the dipping activity is most intense, the low-energy excess has an intensity comparable to that seen during eclipse (Fig. 8*c*). This suggests that during these intervals we are observing X-rays scattered into the line of sight by the ADC. However, during intervals of less intense dipping activity significantly more scattered flux is visible with $\sim 10\%$–20% excess emission. This cannot be coming from the ADC as the eclipse transitions are sharp and flat bottomed which is not consistent with $\sim 10\%$–20% of the emission coming from a region of size $\sim 5 \times 10^{10}$ cm.

c) *Abundance Anomalies*

The absorbed component shows a decrease in normalization during dipping intervals which must reflect energy-independent absorption. We have investigated whether partial ionization of material in the outer regions of the accretion disk would be expected to affect the absorption properties. For the material causing the X-ray intensity dips to be significantly ionized the ionization parameter $\xi = L/nR^2$, where L is the central source luminosity, n is the number density, and r, the distance from the central X-ray source to the clouds, must be > 100 ergs cm s^{-1} (Hatchett, Buff, and McCray 1976). The maximum reduction in intensity during the dips of 80% requires a column, N, of 2.4×10^{24} electrons cm^{-2}. The density is N/l, where l is the length of the column, or $N/\epsilon R$, where ϵ is less than 1. Thus, $\xi > 100$ ergs cm s^{-1} requires that $R < L_{37}\epsilon\ 4.2 \times 10^{10}$ cm, where L_{37} is the central source luminosity in units of 10^{37} ergs s^{-1}. The distance to EXO 0748−676 can be estimated by assuming that the brightest X-ray bursts observed (see Gottwald *et al.* 1986) that do not show radius expansion have a peak luminosity equal to the Eddington luminosity. This implies a distance of 10 kpc and a luminosity of $\sim 1.3 \times 10^{37}$ ergs s^{-1} for the 1985 February 15 observation. The value of ϵ, the depth of the material that produces the dips expressed as a fraction of its distance from the X-ray source, is also poorly known but is likely to be $\ll 1$, and we have adopted a value of 0.1. This implies that material closer than $\sim 5 \times 10^9$ cm from the X-ray source will be significantly ionized. By contrast, the accretion disk is expected to have a radius of $\sim 5 \times 10^{10}$ cm for a 3.8 hr binary period and stellar masses discussed earlier. This requires for partial ionization to be important that the disk is an order of magnitude smaller than expected or that the material responsible for the dips is not located at the edge of the disk, both of which seem unlikely.

It is also unlikely that partial covering of the central source is a factor in determining the absorption properties. We expect the central source to have dimensions comparable to that of a neutron star. This would then require the absorbing cloud size to be smaller than ~ 10 km, and we would expect to observe variability on time scales as short as ~ 0.02 s given a Keplerian velocity at the edge of the disk of ~ 500 km s^{-1}. The shortest time scale at which we see variablity during dipping intervals is ~ 1 s, and while we cannot rule out shorter time scale variations, it seems unlikely that such small-scale structure would exist at the edge of the disk.

The eclipse transition time of ~ 6 s and relative velocity for the two stars of ~ 500 km s^{-1} suggests that either central X-ray source or the obscuring region has a size of ~ 3000 km. If the central X-ray source were to be so big, it might be possible to produce the observed low-energy excess by partial covering. However, it is probable that absorption depth effects in the atmosphere of the companion provide a significant fraction of this extent given the increase in N_H observed during the eclipse transitions. For comparison, a scale height of ~ 100 km is expected for an atmosphere with temperature 4000 K, $\mu = 0.5$, and local gravity 6×10^4 cm s^{-2}, this value being appropriate to the Roche geometry described in Avni and Bahcall (1974) with a system inclination angle of 75°. This means that a 90% reduction in flux will occur at an atmospheric depth of ~ 300 km. This is consistent with the observed extent since the short eclipse duration indicates that the eclipse transition occurs at an angle close to grazing incidence. However, we cannot rule out the possibility that the central source is extended with size < 3000 km. If the source were to be extended, then positional inhomogeneities could be responsible for the spectral changes observed during eclipse transitions.

It is likely that the variation in normalisation of the unabsorbed component is caused by variations in the N_H of the absorbing material for a given count rate. Since the integrations intervals of ~ 1000 s are longer than the characteristic time scale for variability during the dips of ~ 15 s and long term $\sim 30\%$ trends in the source intensity have not been removed, each spectrum includes intervals with differing values of N_H. In order to see whether variations in N_H can produce the observed variation in the normalization of the unabsorbed component we have modeled the absorption assuming that N_H varies in a Gaussian manner around some average value. For an average N_H of 2×10^{22} H cm^{-2} (appropriate to intervals of low dipping activity) it is possible to produce a $\sim 10\%$ low energy excess at 1 keV if N_H has a full width half-maximum of 1×10^{22} H cm^{-2}. During deeper dipping intervals, a similar fractional variation will produce a smaller low-energy excess, consistent with what is observed (Fig. 8*c*).

Comparing the energy independent reduction in flux with that caused by photoelectric absorption allows an estimate of the metallicity of the absorbing material to be made. At the bottom of the deep dips, the residual flux is the same as that seen during eclipse, and the ADC must be responsible for all the residual flux observed. Thus, the results of spectral fits to this data provides an estimate of the abundance that is independent of the origin of the extra unabsorbed emission detected during other dipping intervals. At the bottom of the dips the two component fit gives an N_H of $(1.5^{+1.0}_{-0.5}) \times 10^{23}$ H cm^{-2} with the sum of the normalizations of 0.7 ± 0.1 of that of the quiescent spectrum. This reduction in normalization is similar to that given by the partial covering fits and corresponds to absorption by material that has a metallicity a factor of 2–7 below solar values.

White and Swank (1982) report that the material responsible for the dips observed from XB 1916−053 is underabundant by about a factor of ~ 30 when compared to solar values. Their abundance estimate was obtained by a single component fit to the dip spectra. Figure 7 illustrates how this may lead to an underestimate of the low energy absorption and hence of the metallicity of absorbing elements if a low energy excess is present. It is therefore possible that the metallicity of the material in the XB 1916−053 system is somewhat higher than White and Swank's estimate. The metallicity of the material responsible for the dips seen from X1755−338 is < 600 of that of solar (White *et al.* 1984). The results presented here do not contradict this result since no energy dependence of the X1755−338 spectra is observed, and they cannot be fitted to a variable and fixed absorption component model. As pointed out by White *et al.* (1984) X1755−338 is unlikely to contain an extended central X-ray source since the ratio of X-ray to optical luminosity is $\sim$1000 which is typical of the compact sources associated with Population II companions.

d) *Comparison with Other Systems*

It is interesting to compare the properties of EXO 0748 − 676 with those of X1822 − 371 where only X-rays scattered into the line of sight by an ADC are observed (White *et al.* 1981; White and Holt 1982). The X-ray light curve of X1822 − 371 shows a narrow partial energy-independent dip superposed on a quasi-sinusoidal modulation (Fig. 11). The narrow dip is interpreted as being due to the partial occulation of the extended ADC by the companion star and the underlying modulation by obscuration of the ADC by material in the outer regions of a thick accretion disk. Figure 11 compares the 1–10 keV ME light curves of EXO 0748 − 676 and X1822 − 371 folded over their respective orbital periods. The EXO 0748 − 676 data is taken from the 1985 July 19 observation and the X1822 − 371 data from an *EXOSAT* observation on 1985 May 5 (K. O. Mason 1985, private communication). The remarkable similarity between the light curves of these two very different types of binary systems is evident. This figure illustrates that the principal difference in the two light curves stem from the fact that the central source is hidden by the disk in X1822 − 371. For X1822 − 371 the partial X-ray eclipse is preceeded by a broad minimum which is well modeled in terms of obscuration by a thickened region of the disk (White and Holt 1982). The irregular intensity dips seen from EXO 0748 − 676 range over the same orbital phases as this broad minimum.

In order to model the X-ray light curve of X1822 − 371 White and Holt (1982) required a second thickened region $\sim$100° upstream of a line joining the companion and the compact object. The dips observed at $\phi \approx 0.65$ ($\sim$230° upstream) may be the result of a similar second thickened region in the accretion disk of EXO 0748 − 676. Secondary dips have also been seen from XB 1916 − 053 (White and Swank 1982; Walter *et al.* 1982) which require the presence of a second thickened region in the disk $\sim$180° upstream. The origin of this additional structure is probably from a second impact point or splash of material that is deflected following the initial

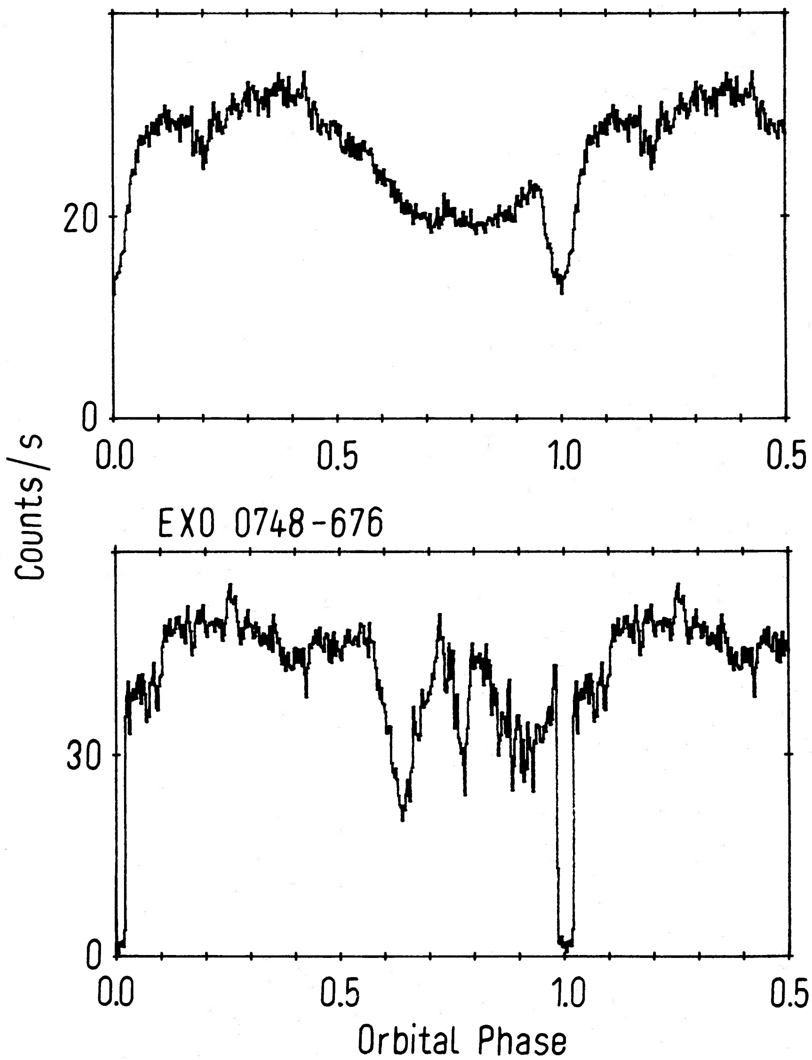

FIG. 11.—The folded 1–10 keV ME light curves of X1822 − 371 (*upper panel*) and EXO 0748 − 676 data is from the observation on 1985 July 19 and is folded using the ephemeris given in the text. The X1833 − 371 data is from a 18 hr duration *EXOSAT* observation that started on 1985 May 5 at 0.7 hr and is folded using the period given in White *et al.* (1981) with phase chosen to align the partial eclipse with $\phi = 0$ for EXO 0748 − 676.

TABLE 2

SYSTEM INCLINATIONS AND COMPANION MASSES

System	Inclination Angle	Mass ($M_\odot$)	X-Ray Source	Reference
EXO 0748−676	75°–83°	0.45–0.08	Point	This work
XBT 1659−298	72–90	0.9–0.25	Point	Cominsky and Wood 1984
X1822−371	75–85	0.5–0.08	Extended	White and Holt 1982
XT 2129+470	80–90	0.65–0.2	Extended	White and Holt 1982; McClintock *et al.* 1982

impact. The position of this second splash may vary depending on the mass ratio of the system.

XBT 1659−298 also shows irregular intensity dips during ~25% of its 7.1 hr orbital cycle followed by a 15 minute stable dip (Cominsky and Wood 1984) which these authors suggest is probably an eclipse by the companion star. These *EXOSAT* observations support this suggestion since the phasing and eclipse semiangle of the stable dip from XBT 1659−298 and the eclipse of EXO 0748−676 are similar. For comparison Table 2 gives the allowed ranges of companion mass and system inclinations for XBT 1659−298, X1822−371, and XT 2129+470 as well as for EXO 0748−676 derived using eclipse duration measurements. It can be seen that for the assumption of main-sequence companions the inclination angles of the dipping and partial eclipsing ADC systems are similar. This means that in the latter systems that either the accretion disks must be thicker or that the companions are oversized for their masses.

It is interesting to note that out of the seven LMXRB systems that are known to exhibit periodic intensity dips, the only systems to also show eclipses are also transients. This could be coincidental, but it might suggest that the transient nature of these particular sources is related to the inclination angle.

The detection of low level emission from EXO 0748−676 by the *Einstein* IPC in 1980 suggests that EXO 0748−676 undergoes intervals when it is a much fainter X-ray source. At these times the accretion disk may completely hide the central X-ray source and the source would be similar to X1822−371, XT 2129+470, and also Hercules X-1 in its extended low state (Parmar *et al.* 1985*a*) where only low-level scattered X-rays are visible. Given that the inclination angles of EXO 0748−676 and X1822−371 are so similar (Table 2), presumably only a small change in disk thickness would be required. Alternatively EXO 0748−676 could be an intrinsically low-level X-ray source between outbursts. We note that there is no an object brighter than $m_v \approx 22$ at the position of EXO 0748−676 on the SRC *J* survey plate of the region (Wade *et al.* 1985) implying that at times EXO 0748−676 is extremely faint. It is of interest to continue to monitor this source optically and to study it in a faint state.

e) A γ-Ray Burst Source?

As noted by Pedersen *et al.* (1985) EXO 0748−676 lies within the 3° × 3° γ-ray error region of GB 811016 (Katoh *et al.* 1984) determined from *Hakucho* data alone. However, it lies more than 10 times the half-width away from the revised joint *Hakucho-Pioneer Venus Orbiter-International Cometary Explorer* timing position anulus (Laros *et al.* 1985). We conclude that the original positional coincidence was fortuitous and that EXO 0748−676 and the nearby γ-ray source are not related.

IX. CONCLUSION

We have discovered a new transient X-ray binary system that shows a remarkably rich range of phenomena including eclipses, intensity dips, and X-ray bursts. Detailed modeling of the spectra obtained during the dips show that the material responsible for the dipping activity has a metallicity a factor of 2–7 below solar values. The dip spectra and residual emission seen during eclipse suggest the presence of an extended emission region in the system with radius $\sim 5 \times 10^{10}$ cm which contributes ~4% of the total observed 2–10 keV X-ray intensity. We observe clear evidence for an evolution of the X-ray light curve as the outburst evolved, some of the effects of which may be related to mass accretion rate.

We thank K. O. Mason for communicating the X1822−371 results prior to publication and T. Maccacaro for assistance with the *Einstein* analysis. A Peacock and B. G. Taylor are thanked for their support and the *EXOSAT Observatory* team for help with these observations.

REFERENCES

Avni, Y., and Bahcall, J. N. 1975, *Ap. J.*, **197**, 675.
Bode, M. F., Priedhorsky, W. C., Norwell, G. A., and Evans, A. 1985, *Ap. J.*, **299**, 845.
Catura, R. C. 1983, *Ap. J.*, **275**, 645.
Cominsky, L. R., and Wood, K. S. 1984, *Ap. J.*, **283**, 765.
Courvoisier, T., Parmar, A. N., and Peacock, A. 1984, in *Proc. X-ray Symposium* (Bologna), ed. M. Oda and R. Giacconi (Tokyo: Institute of Space and Astronautical Science), p. 153.
Crampton, D., Cowley, A. P., Stauffer, J., Ianna, P., and Hutchings, J. B. 1986, *Ap. J.*, **306**, 599.
de Korte, P. A. J., *et al.* 1981, *Space Sci. Rev.*, **31**, 495.
Doty, J. 1976, *IAU Circ.*, 2922.
Forman, W., Jones, C., Cominsky, L., Julien, P., Murray, S., Peters, G., Tananbaum, H., and Giacconi, R. 1978, *Ap. J. Suppl.*, **83**, 357.
Gottwald, M., Haberl, F., Parmar, A. N., and White, N. E. 1986, *Ap. J.*, **308**, 213.
Hatchett, S., Buff, J., and McCray, R. 1976, *Ap. J.*, **206**, 847.
Katoh, M., Murakami, T., Nishimura, J., Yamagami, T., Fujii, M., and Itoh, M. 1984, *AIP Conference Proc.*, **115**, 390.
Laros, J. G., Fenimore, E. E., Fikani, M. N., and Klebesadel, R. W. 1985, *IAU Circ.*, 4054.
Mason, K. O., and Córdova, F. 1982, *Ap. J.*, **255**, 603.
Mason, K. O., Parmar, A. N., and White, N. E. 1985, *M.N.R.A.S.*, **216**, 1033.
Mauche, C. W., and Gorenstein, P. 1986, *Ap. J.*, **302**, 371.
McClintock, J. E., London, R. A., Bond, H. E., and Grauer, A. D. 1982, *Ap. J.*, **258**, 245.
McHardy, I., Lawrence, A., Pye, J. P., and Pounds, K. 1981, *M.N.R.A.S.*, **197**, 893.
Morrison, R., and McCammon, D. 1983, *Ap. J.*, **270**, 119.
Motch, C., Pedersen, H., Ilovaisky, S., Chevalier, C., and Pakull, M. W. 1984, in *Proc. X-ray Symposium* (Bologna), ed. M. Oda and R. Giacconi (Tokyo: Institute of Space and Astronautical Science), p. 149.
Mouchet, M., Angebault, L. P., and Ilovaisky, S. A. 1985, *IAU Circ.*, 4076.
Nagase, F. 1985, in *Galactic and Extragalactic Compact X-ray Sources*, ed. Y. Tanaka and W. H. G. Lewin (Tokyo: Institute of Space and Astronomical Science), p. 7.
Overbeck, J. W. 1965, *Ap. J.*, **141**, 864.
Paczyński, B. 1971, *Ann. Rev. Astr. Ap.*, **9**, 183.

Parmar, A. N., Pietsch, W., McKechnie, S., White, N. E., Trumper, J., Voges, W., and Barr, P. 1985*a*, *Nature*, **313**, 119.
Parmar, A. N., White, N. E., Giommi, P., and Haberl, F. 1985*b*, *IAU Circ.*, **4039**.
Peacock, A., Andresen, R. D., Manzo, G., Taylor, B. G., Villa, G., Ives, J. C., and Kellock, S. 1981, *Space Sci. Rev.*, **30**, 525.
Pedersen, H., Cristiani, S., d'Ororico, S., and Thomsen, B. 1985, *IAU Circ.*, 4047.
Pedersen, H., and Mayor, M. 1985, *IAU Circ.*, 4039.
Rolf, D. P. 1983, *Nature*, **302**, 46.
Turner, M., Smith, A., and Zimmermann, H. U. 1981, *Space Sci. Rev.*, **30**, 513.
van der Klis, M., Parmar, A. N., van Paradijs, J., Jansen, F., and Lewin, W. H. G. 1985, *IAU Circ.*, 4044.
Wade, R. A., Quintana, H., Horne, K., and March, T. R. 1985, *Pub. A.S.P.*, **97**, 1092.
Walter, F. M., Bowyer, S., Mason, K. O., Clarke, J. T., Henry, J. P., Halpern, J., and Grindlay, J. E. 1982, *Ap. J.* (*Letters*), **253**, L67.
Watson, M. G., Willingale, R., King, A. R., Grindlay, J. E., and Halpern, J. E. 1985, *IAU Circ.*, 4051.
White, N. E., Becker, R. H., Boldt, E. A., Holt, S. S., Serlemitsos, P. J., and Swank, J. H. 1981, *Ap. J.*, **247**, 994.
White, N. E., and Holt, S. S. 1982, *Ap. J.*, **257**, 318.
White, N. E., and Mason, K. O. 1985, *Space Sci. Rev.*, **40**, 167.
White, N. E., Parmar, A. N., Sztajno, M., Zimmermann, H. U., Mason, K. O., and Kahn, S. M. 1984, *Ap. J.* (*Letters*), **283**, L9.
White, N. E., and Swank, J. H. 1982, *Ap. J.* (*Letters*), **253**, L61.
Whyte, C. A., and Eggleton, P. 1980, *M.N.R.A.S.*, **190**, 801.
Wood, K. S., *et al.* 1984, *Ap. J. Suppl.*, **56**, 507.
Xu, Y., McCray, R., and Kelley, R. 1986, *Nature*, **319**, 652.

Paolo Giommi, Manfred Gottwald, Arvind N. Parmar, and Nick E. White: EXOSAT Observatory, ESOC, Robert Bosch Strasse 5, 6100 Darmstadt, W. Germany